Doppler Stretch Estimation with Application to Tracking Globalstar Satellite Signals

Mohammad Neinavaie*, Joe Khalife*, and Zaher M. Kassas*†
* Department of Mechanical and Aerospace Engineering
† Department of Electrical Engineering and Computer Science
University of California, Irvine
{mneinava@uci.edu, kalifej@uci.edu, zkassas@ieee.org}

***Abstract*—Tracking the Doppler frequency of a transmitter, where the Doppler is being compensated at the transmitter is considered. A particular example where this occurs is Globalstar low Earth orbit (LEO) satellites. Doppler compensation takes place based on the center of each satellite transmitter beams. When the Doppler is compensated, the measured Doppler by a ground receiver is different from the real Doppler, which renders the measured Doppler unusable for applications such as opportunistic navigation. This paper presents an approach to estimate the true (i.e., uncompensated) Doppler, which is subsequently used for code and carrier phase tracking. Experimental results are presented of the first delay tracking with real Globalstar satellite signals, showing the proposed technique closely matching the tracking predicted by two-line element (TLE) files.**

I. Introduction

Signals of opportunity (SOPs), whether terrestrial or space-based, have been considered as complements or alternatives to global navigation satellite system (GNSS) signals [1]. In particular, the promise of utilizing low Earth orbit (LEO) satellites for navigation has been the subject of several studies, with increased attention in the past few years [2]–[11]. While some of these studies require tailoring the broadband protocol to support navigation capabilities [12], [13], other studies propose to exploit existing and future broadband LEO constellations for navigation in an opportunistic fashion [14]–[19]. Tailoring the existing broadband protocols to support navigation capabilities allow for simpler receiver architectures and navigation algorithms. However, they require significant changes to existing infrastructure, the cost of which private companies such as OneWeb, SpaceX, Boeing, and others, which are planning to launch tens of thousands of broadband Internet satellites into LEO, may not be willing to pay.

LEO satellites possess desirable attributes for positioning in GNSS-challenged environments: (i) they are around twenty times closer to Earth compared to GNSS satellites, which reside in medium Earth orbit (MEO), making their received signal power between 24 to 34 dBs higher than GNSS signals; (ii) they will become abundant as tens of thousands of broadband Internet satellites are expected to be deployed into LEO; and (iii) each broadband provider will deploy satellites into unique constellations, transmitting at different frequency bands, making LEO satellite signals diverse in frequency and direction. Using two-line element (TLE) files and orbit determination algorithms (e.g., SGP4), the positions and velocities of these satellites can be estimated, albeit not precisely. In addition, some of these broadband LEO satellites, such as Orbcomm satellites, are equipped with GPS receivers and broadcast their GPS solution to terrestrial receivers.

One of the main challenges to navigate exclusively with LEO satellite signals is that their signal specifications may not be available to the public, which makes acquiring and tracking these signals impossible for conventional opportunistic navigation receivers. In particular, the Globalstar satellite system [20] supposedly uses a similar protocol to the IS-95 and cdma2000 cellular code-division multiple access (CDMA) system but with different pseudo-noise (PN) sequences [21]. It should be noted that since Globalstar is a bent-pipe satellite system [22], the signaling characteristics might be updated during the course of time. A blind opportunistic navigation framework was presented in [23]–[25] to exploit partially known sources for navigation purposes.

This paper considers Globalstar satellite signals. To the best of the author's knowledge, this paper shows the first tracking results of Globalstar signals. One of the challenges of opportunistic navigation with Globlastar satellites is *Doppler compensation*. In Globalstar LEO satellite system, the Doppler is compensated to a nominal value at the satellite or at the ground station [21]. Doppler compensation takes place based on the center of each satellite transmitter beams. When the Doppler is compensated, the measured Doppler by a ground receiver is different from the real Doppler, which renders the measured Doppler unusable for opportunistic navigation. This paper utilizes spectrum distortion to recover the Doppler frequency and track Globalstar satellite signals. The idea behind the presented method is that even though the Doppler is compensated, it can be be estimated coarsely at the receiver, based on the time compression or expansion of the received signal due to the original Doppler. This compression/expansion effect changes the apparent chipping rate at the receiver and distorts the spectrum of the transmitted signal.

The rest of the paper is organized as follows. Section II describes the received baseband signal model. Section III presents the proposed approach to track Globalstar signals, while estimating the Doppler stretch. Section IV presents experimental results. Section V gives concluding remarks.

This work was supported in part by the Office of Naval Research (ONR) under Grant N00014-19-1-2511 and Grant N00014-19-1-2613.

II. Signal Model

Consider a LEO satellite that moves with a constant radial velocity v relative to the receiver. The velocity is positive if the LEO satellite moves away from the receiver. Thus, the distance between the LEO satellite and the receiver is $r(t) = r(0) + vt$. Denote the transmitted signal by $p(t)\exp(j\omega_c t)$, where $p(t)$ is a waveform, $\omega_c = 2\pi f_c$, and f_c is the carrier frequency. The received signal can be modeled as

$$y(t) = \alpha p(t - \tau(t))\exp\left[j\omega_c(t - \tau(t))\right] + w(t), \quad (1)$$

where α is the channel gain, $w(t)$ is an additive noise, and

$$\tau(t) = \frac{r(t)}{c} = t_0 + \gamma t, \quad (2)$$

where $t_0 \triangleq \frac{r(0)}{c}$, $\gamma \triangleq \frac{v}{c}$ is the Doppler stretch, and c is the speed of light. Hence, the received signal can be written as

$$y(t) = \alpha' p\left[(1-\gamma)t - t_0\right]\exp(-j2\pi f_D t)\exp\left(j\omega_c t\right) + w(t), \quad (3)$$

where $f_D = f_c\gamma$ is the Doppler frequency, and $\alpha' = \alpha\exp\left(-j\omega_c t_0\right)$ is the equivalent channel gain. It can be inferred from (3) that the Doppler effect results in the time expansion or time compression of the transmitted signal. In other words, the relative velocity of the transmitter and the receiver results in two changes in the characteristics of the transmitted signal: (i) the phase which appears as the Doppler frequency shift and (ii) the time scale which appears as time expansion or time compression. However, in some applications, the expansion or compression is negligible. More precisely, denoting the bandwidth and the duration of the transmitted signal by B and T, respectively, if

$$BT \ll \frac{c}{2|v|}, \quad (4)$$

the stretching effect can be neglected [26], i.e., (3) can be approximated as

$$y(t) \approx \alpha' p(t - t_0)\exp(-j2\pi f_D t)\exp\left(j\omega_c t\right) + w(t), \quad (5)$$

which is referred to as the narrow-band model for the transmitted signal. Intuitively, a periodic signal can be considered as a linear combination of constant frequency complex exponential components, i.e., $\exp(j2\pi ft)$, where f is within the bandwidth of the transmitted signal. For each complex exponential component, the Doppler changes the carrier frequency by $|\gamma|f$, which results in the variation of phase rotation over the signal duration of $\frac{T}{1-\gamma}$ by $2\pi|\gamma|fT/(1-\gamma)$. Hence, $2|v|BT/c \ll 1$ should hold in order for the variations of the phase rotations for all the complex exponential components to be equal.

A. Globalstar Forward Link Signals

Globalstar LEO satellites employ CDMA. For a given Forward CDMA Channel, the spreading and modulation process is applied as shown in Fig. 1. The spreading sequence structure is comprised of an inner PN sequence pair and an outer PN sequence. The inner sequence has a chip rate of $R_{c_{in}} = 1.2288$ Mcps and a length of $L_{c_{in}} = 2^{10}$ chips. The outer PN sequence has 1200 outer chips per second and a length of 288 outer PN chips. One inner PN sequence period exactly fits into a single outer PN chip. The outer PN modulates the inner PN sequence to produce the actual spreading sequence resulting in a period of 240 ms. It should be noted that the inner PN sequence pair identifies the satellite orbital plane; there are eight different pairs. The outer PN sequence identifies the satellite. Each satellite beam is identified by a time offset of the outer PN sequence for the corresponding orbit. The gateways perform precorrection of time and frequency in their transmitted waveform to compensate for time delay and Doppler variations due to satellite motion for the feeder link. Considering inner and outer PN sequences, the overall length of PN sequence for Globalstar signals is $L_c = 288 \times 2^{10}$ chips an the period of the PN sequence is $T_c = 0.24$ s. However, accroding to (3), and due to the high speed of the LEO satellites relative to the receiver, the apparent period of the transmitted signal at the receiver might be different from T_c. This is due to the time expansion or time compression effect.

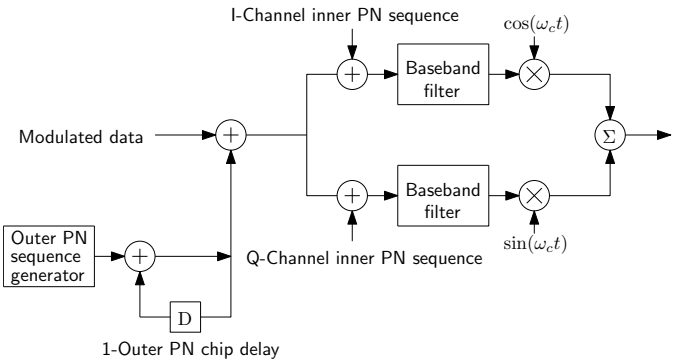

Fig. 1. Block diagram of forward link spreading in Globalstar CDMA based downlink signals. In this diagram the + sign is used to show the spreading operation [21].

Remark 1: According to (3), the apparent period is $T_{c_{\text{app}}} = \frac{T_c}{1-\gamma}$ and, consequently, the apparent chipping rate is $R_{c_{\text{app}}} = R_c - \epsilon$, where $\epsilon = \gamma R_c$ hereafter is referred to as chipping rate offset (CRO).

It should be pointed out that the relation ship between the CRO and the Doppler is $\epsilon = \frac{R_c}{f_c} f_D$. For instance, for a transmitted signal at carrier frequency 2481.77 MHz with a chipping rate of $R_c = 1.2288$ MHz and a Doppler frequency of 20 kHz will result in $\epsilon \approx 10$ Hz.

Assuming that the sampling frequency is F_s, the number of samples of one period of the PN sequence is $N_c = \frac{L_c}{R_c} Fs$. Therefore, the apparent number of samples of the PN sequence is

$$N_{c_{\text{app}}} = \frac{N_c R_c}{R_c - \epsilon} = \frac{L_c F_s}{R_c - \epsilon}. \quad (6)$$

Factorizing R_c, expanding the Taylor series results around $\epsilon = 0$, and retaining the first terms results in

$$N_{c_{\text{app}}} \approx \frac{L_c F_s}{R_c}\left(1 - \frac{\epsilon}{R_c}\right). \quad (7)$$

Therefore, the apparent number of samples of the PN sequence will change by

$$k = \left\lfloor \frac{N_c F_s \epsilon}{R_c^2} \right\rceil \tag{8}$$

samples, where $\lfloor \cdot \rceil$ denotes rounding to the closest integer.

III. Chipping Rate Offset Estimation

As mentioned previously, due to the high Doppler frequencies of LEO satellites, the apparent chipping rate can be different from its original value and the difference between these two values is referred to as the CRO.

A. Doppler compensation

In a wideband communication system, when the bandwidth and signal duration do not satisfy (4), the narrowband signal model (5) will not hold and conventional Doppler and delay estimation/tracking schemes will not work properly [26]. Hence, a Doppler tracking algorithm should be aided by a CRO estimator. In this paper, another motivation for CRO estimation is presented. In some LEO satellites, the Doppler is corrected/compensated at the gateway [21]. *Doppler compensation* is performed to reduce the apparent Doppler frequency at the user terminals. Using phased array antennas, *spot beams* can be used to enhance coverage and reduce interference. Doppler compensation can be performed at the gateway according to the center of a spot beam (see Fig. 2). Therefore, the user will experience a Doppler which is different from f_D in (3). Hence, the estimated Doppler will not match with that of the TLE files.

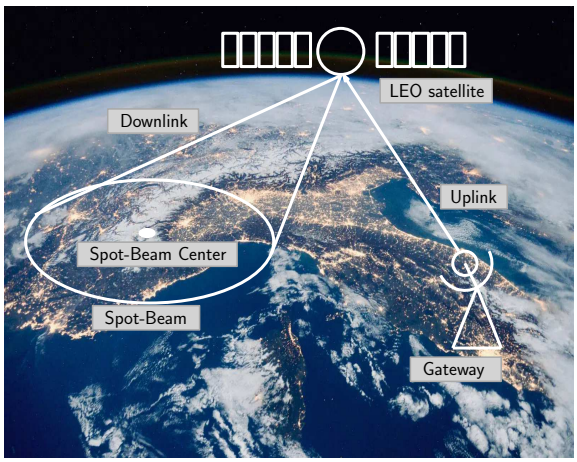

Fig. 2. Gateway to user terminal link and the spot beam.

B. Recovering the Original Doppler Frequency

Denoting the estimated Doppler of the center of spot beam at the gateway by $\hat{f}_{D_G}$, the received signal model can be expressed as

$$y(t) = \alpha' p\left[(1-\gamma)t - t_0\right] \exp\left[-j2\pi\left(f_D - \hat{f}_{D_G}\right)t\right] \cdot \exp\left(j\omega_c t\right) + w(t). \tag{9}$$

After carrier wipe-off and sampling, the discrete-time model can be expressed as

$$y[n] = \alpha' p[(1-\nu)n - n_0] \exp\left(j2\pi \frac{f_D - \hat{f}_{D_G}}{F_s} n\right) + w[n]. \tag{10}$$

Consequently, a Doppler estimator yields an estimate of the *compensated* Doppler, i.e., $f_D - \hat{f}_{D_G}$, rather than the *true* Doppler. It should be pointed out that γ still contains the effect of the Doppler frequency. Therefore, estimating γ provides an estimate of the Doppler frequency according to $f_D = \gamma f_c$. The maximum likelihood estimator is used to estimate ϵ and consequently the PN sequence. The detected PN sequence was used to acquire and track the Globlstar satellite signal using the receiver implementation discussed in [27]. It should be pointed out that the detected PN sequence has a time-varying length. In other words, the length of the PN sequence depends of the Doppler frequency which changes with time. Therefore, the main difference between the proposed receiver and the CDMA receiver presented in [27] is that the delay estimation is performed using the PN sequence with the apparent length.

C. CRO-Aided Tracking Loops

After obtaining an estimate of γ, phase-locked loops (PLLs) are employed to track the carrier phases of the detected satellite and carrier-aided delay-locked loops (DLLs) are used to track the code phase of the PN sequence. Fig. 3 shows the block diagram of the CRO-aided tracking loops.

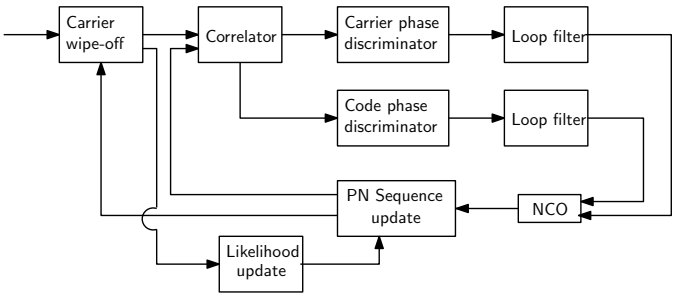

Fig. 3. Block diagram of CRO-aided tracking loops.

Using a maximum-likelihood (ML) estimator of γ, the apparent chipping rate of the locally generated PN sequence is adjusted according to $R_{c_{rmapp}} = R_c - \epsilon$.

The PLL consists of a phase discriminator, a loop filter, and a numerically-controlled oscillator (NCO). It was found that the receiver could track the carrier phase with a second-order PLL with a loop filter transfer function

$$F_{\mathrm{PLL}}(s) = \frac{2\kappa\omega_n s + \omega_n^2}{s}, \tag{11}$$

where $\kappa \equiv \frac{1}{\sqrt{2}}$ is the damping ratio and ω_n is the undamped natural frequency, which can be related to the PLL noise-equivalent bandwidth $B_{n,\mathrm{PLL}}$ by $B_{n,\mathrm{PLL}} = \frac{\omega_n}{8\zeta}(4\zeta^2+1)$ [28]. The loop filter transfer function in (11) is discretized at a sampling period $T_{\mathrm{sub}} \triangleq \frac{L_c}{F_s}$, which is the time interval at which the loop filters are updated and is typically known as the

subaccumulation interval. The discretized transfer function is realized in state-space. The output of the loop filter at time-step k, denoted by $v_{\mathrm{PLL},k}$, is the rate of change of the carrier phase error, expressed in rad/s. The Doppler frequency estimate at time-step k is deduced by dividing $v_{\mathrm{PLL},k}$ by 2π. The carrier phase estimate at time-step k is updated according to

$$\hat{\theta}_k = \hat{\theta}_{k-1} + v_{\mathrm{PLL},k} \cdot T_{\mathrm{sub}}, \tag{12}$$

where $\hat{\theta}_0 \equiv 0$.

The carrier-aided DLL employs an early-minus-late discriminator. The early and late correlations at time-step k used in the discriminator are denoted by Z_{e_k} and Z_{l_k}, respectively, which are calculated by correlating the received signal with an early and a delayed version of the estimated PN sequence, respectively. The time shift between Z_{e_k} and Z_{l_k} is defined as the early-minus-late time, denoted by ξ. The DLL loop filter is a simple gain K_{DLL}, with a noise-equivalent bandwidth $B_{n,\mathrm{DLL}} = \frac{K_{\mathrm{DLL}}}{4} \equiv 0.5$ Hz. The output of the DLL loop filter v_{DLL} is the rate of change of the code phase, expressed in s/s. Assuming low-side mixing at the radio frequency front-end, the code phase estimate is updated according to

$$\hat{t}_{s_{k+1}} = \hat{t}_{s_k} - \left(v_{\mathrm{DLL},k} + \frac{v_{\mathrm{PLL},k}}{2\pi f_c} \right) \cdot T_{\mathrm{sub}}. \tag{13}$$

The code phase estimate can be used to deduce the pseudorange observables.

IV. Experimental Results

This section validates the proposed receiver experimentally. The objective of these experiments are to: (i) compare the measured Doppler with the Doppler from the TLE files to visualize the Doppler compensation effect and (ii) compare the variation in the pseudorange estimated by the receiver to the variation in range between the stationary receiver and the Globalstar satellites obtained by the TLE files. For this purpose, the stationary receiver was equipped with a costumer-grade GAT-17MP Globalstar antenna and a small consumer-grade GPS. The satellite signals were down-mixed and sampled via a single-channel universal software radio peripheral (USRP) 2974 driven by a GPS-disciplined oscillator (GPSDO). Fig. 4 illustrates the experimental setup. Samples of the received signals were stored for off-line post-processing.

Fig. 5 demonstrates the estimated Doppler by the receiver and the Doppler obtained from the TLE files. It can be seen that the measured Doppler is dramatically different from the Doppler profile obtained from the TLE files. As mentioned previously, Doppler compensation is performed to reduce the apparent Doppler frequency at the user terminals. Doppler compensation is performed at the gateway according to the center of the spot beam. Due to the distance between the center of the spot beam and the user terminal, the user terminal experiences a Doppler frequency which is relatively smaller than what is expected from the Doppler from the TLE files.

The CRO ϵ is estimated and used to estimate the transmitted PN sequence. The likelihood function of the ML estimator for different values of ϵ is demonstrated in Fig. 6. The estimated

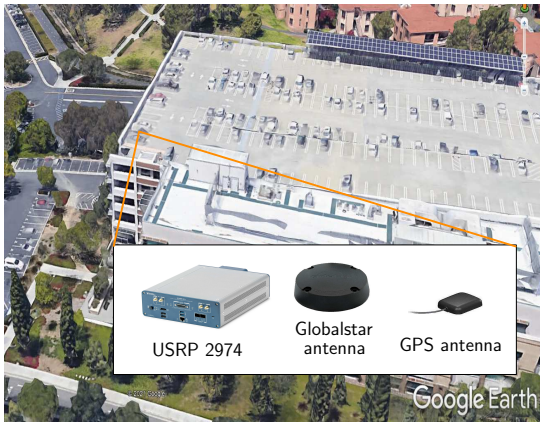

Fig. 4. Experimental setup.

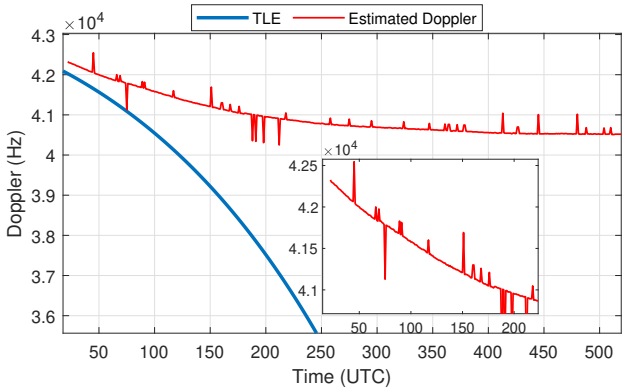

Fig. 5. The estimated Doppler frequency and the Doppler obtained from TLE files.

PN sequence was used to acquire and track the Globlstar satellite using the receiver implementation discussed in [27]. The tracking tracking results versus those obtained from TLE are plotted in Fig. 7.

As can be seen from this figure, the proposed method is tracking the pseudorange of one of Globalstar satellites which was available in a window of 190 s at the time of experiment. The average error between the measured pseudornage and the pseudorange predicted is approximately 111.12 m over a window of 190 s.

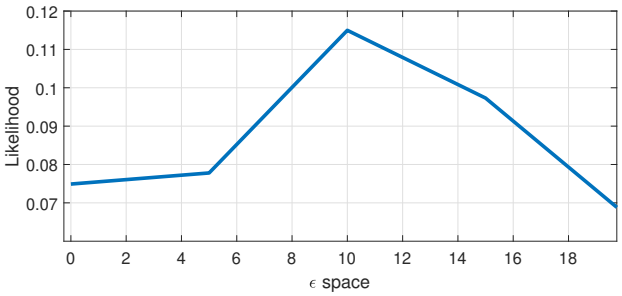

Fig. 6. The likelihood function for the ML estimator of Globalstar forward link signals for different values of epsilon.

(a)

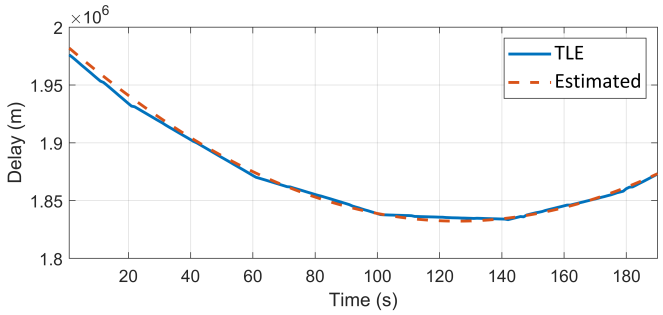

(b)

Fig. 7. (a) Trajectory of Globalstar satellite GS 37743. (b) Comparing the delay tracking results obtained by the proposed receiver with the delays obtained from the TLE.

V. Conclusion

This paper considered the problem of tracking LEO satellites in a scenarios where the Doppler is changed or *compensated* for at the transmitter. One example of a compensated Doppler is the Globalstar LEO satellite forward link signals. This paper presented a Doppler stretch estimation technique to enable the tracking of Globalstar satellite signals. Experimental results were presented showing close match between the proposed delay tracking technique versus the delay predicted by TLE files.

References

[1] J. Raquet *et al.*, "Position, navigation, and timing technologies in the 21st century," J. Morton, F. van Diggelen, J. Spilker, Jr., and B. Parkinson, Eds. Wiley-IEEE, 2021, vol. 2, Part D: Position, Navigation, and Timing Using Radio Signals-of-Opportunity, ch. 35–43, pp. 1115–1412.

[2] M. Rabinowitz, "A differential carrier-phase navigation system combining GPS with low Earth orbit satellites for rapid resolution of integer cycle ambiguities," Ph.D. dissertation, Stanford University, USA, 2000.

[3] M. Joerger, L. Gratton, B. Pervan, and C. Cohen, "Analysis of Iridium-augmented GPS for floating carrier phase positioning," *NAVIGATION, Journal of the Institute of Navigation*, vol. 57, no. 2, pp. 137–160, 2010.

[4] D. Lawrence, H. Cobb, G. Gutt, M. OConnor, T. Reid, T. Walter, and D. Whelan, "Navigation from LEO: Current capability and future promise," *GPS World Magazine*, vol. 28, no. 7, pp. 42–48, July 2017.

[5] T. Reid, A. Neish, T. Walter, and P. Enge, "Broadband LEO constellations for navigation," *NAVIGATION, Journal of the Institute of Navigation*, vol. 65, no. 2, pp. 205–220, 2018.

[6] T. Reid, K. Gunning, A. Perkins, S. Lo, and T. Walter, "Going back for the future: Large/mega LEO constellations for navigation," in *Proceedings of ION GNSS Conference*, September 2019, pp. 2452–2468.

[7] Z. Kassas, J. Morales, and J. Khalife, "New-age satellite-based navigation – STAN: simultaneous tracking and navigation with LEO satellite signals," *Inside GNSS Magazine*, vol. 14, no. 4, pp. 56–65, 2019.

[8] R. Morales-Ferre, E. Lohan, G. Falco, and E. Falletti, "GDOP-based analysis of suitability of LEO constellations for future satellite-based positioning," in *Proceedings of IEEE International Conference on Wireless for Space and Extreme Environments*, 2020, pp. 147–152.

[9] S. Thompson, S. Martin, and D. Bevly, "Single differenced doppler positioning with low Earth orbit signals of opportunity and angle of arrival estimation," in *Proceedings of ION International Technical Meeting*, 2020, pp. 497–509.

[10] T. Reid, T. Walter, P. Enge, D. Lawrence, H. Cobb, G. Gutt, M. O'Conner, and D. Whelan, "Position, navigation, and timing technologies in the 21st century," J. Morton, F. van Diggelen, J. Spilker, Jr., and B. Parkinson, Eds. Wiley-IEEE, 2021, vol. 2, ch. 43: Navigation from low Earth orbit – Part 1: Concept, Current Capability, and Future Promise, pp. 1359–1379.

[11] M. Psiaki, "Navigation using carrier doppler shift from a LEO constellation: TRANSIT on steroids," *NAVIGATION, Journal of the Institute of Navigation*, vol. 68, no. 3, pp. 621–641, September 2021.

[12] P. Iannucci and T. Humphreys, "Economical fused LEO GNSS," in *Proceedings of IEEE/ION Position, Location and Navigation Symposium*, 2020, pp. 426–443.

[13] T. Reid, B. Chan, A. Goel, K. Gunning, B. Manning, J. Martin, A. Neish, A. Perkins, and P. Tarantino, "Satellite navigation for the age of autonomy," in *Proceedings of IEEE/ION Position, Location and Navigation Symposium*, 2020, pp. 342–352.

[14] Z. Tan, H. Qin, L. Cong, and C. Zhao, "New method for positioning using IRIDIUM satellite signals of opportunity," *IEEE Access*, vol. 7, pp. 83 412–83 423, 2019.

[15] J. Khalife, M. Neinavaie, and Z. Kassas, "Navigation with differential carrier phase measurements from megaconstellation LEO satellites," in *Proceedings of IEEE/ION Position, Location, and Navigation Symposium*, April 2020, pp. 1393–1404.

[16] F. Farhangian and R. Landry, "Multi-constellation software-defined receiver for Doppler positioning with LEO satellites," *Sensors*, vol. 20, no. 20, pp. 5866–5883, October 2020.

[17] M. Orabi, J. Khalife, and Z. Kassas, "Opportunistic navigation with Doppler measurements from Iridium Next and Orbcomm LEO satellites," in *Proceedings of IEEE Aerospace Conference*, March 2021, pp. 1–9.

[18] F. Farhangian, H. Benzerrouk, and R. Landry, "Opportunistic in-flight INS alignment using LEO satellites and a rotatory IMU platform," *Aerospace*, vol. 8, no. 10, pp. 280–281, 2021.

[19] J. Khalife, M. Neinavaie, and Z. Kassas, "The first carrier phase tracking and positioning results with Starlink LEO satellite signals," *IEEE Transactions on Aerospace and Electronic Systems*, 2021, accepted.

[20] R. Hendrickson, "Globalstar for the military," in *Proceedings of IEEE Military Communications Conference*, vol. 3, November 1997, pp. 1173–1178.

[21] L. Schiff and A. Chockalingam, "Signal design and system operation of Globalstar TM versus IS-95 CDMA – Similarities and differences," *Wireless Networks*, vol. 6, no. 1, pp. 47–57, February 2000.

[22] M. Rabinowitz, B. Parkinson, C. Cohen, M. O'Connor, and D. Lawrence, "A system using LEO telecommunication satellites for rapid acquisition of integer cycle ambiguities," in *Proceedings of IEEE/ION Position Location and Navigation Symposium*, April 1998, pp. 137–145.

[23] M. Neinavaie, J. Khalife, and Z. Kassas, "Blind opportunistic navigation: Cognitive deciphering of partially known signals of opportunity," in *Proceedings of ION GNSS Conference*, September 2020, pp. 2748–2757.

[24] J. Khalife, M. Neinavaie, and Z. Kassas, "Blind Doppler estimation from LEO satellite signals: A case study with real 5G signals," in *Proceedings of ION GNSS Conference*, September 2020, pp. 3046–3054.

[25] M. Neinavaie, J. Khalife, and Z. Kassas, "Blind Doppler tracking and beacon detection for opportunistic navigation with LEO satellite signals," in *Proceedings of IEEE Aerospace Conference*, March 2021, pp. 1–8.

[26] T. Zhao and T. Huang, "Cramer-Rao lower bounds for the joint delay-Doppler estimation of an extended target," *IEEE Transactions on Signal Processing*, vol. 64, no. 6, pp. 1562–1573, 2016.

[27] J. Khalife, K. Shamaei, and Z. Kassas, "Navigation with cellular CDMA signals – part I: Signal modeling and software-defined receiver design," *IEEE Transactions on Signal Processing*, vol. 66, no. 8, pp. 2191–2203, April 2018.

[28] P. Misra and P. Enge, *Global Positioning System: Signals, Measurements, and Performance*, 2nd ed. Ganga-Jamuna Press, 2010.